

Dual Space Approach to the Classification of Toroidal Carbon Nanotubes

Chern Chuang, Yuan-Chia Fan, and Bih-Yaw Jin*

Department of Chemistry, Center for Theoretical Sciences, and Center for Quantum Science and Engineering,
National Taiwan University, Taipei, Taiwan, ROC

Received April 3, 2009

We apply the dual space approach to the classification of toroidal carbon nanotubes. We show that the realizations of most of the geometric manipulations described in the literature become explicit in the dual space of the original molecular graph. In particular, dual graph can be easily constructed on a rectangular strip in the parametric plane of the torus. Generalization to other forms of graphitic cages with different topologies can also be done. Manifested chirality and the criteria for the existence of highly symmetric isomers are discussed.

INTRODUCTION

Since the advance of fullerene science^{1,2} and subsequent boom of research papers on the interesting physical properties of them, materials made of pure sp² carbon network are of intense interest among scientific society in the last two decades. Among them, molecules with toroidal shape may have particularly intriguing properties because of their exotic geometries and topology. Toroidal carbon nanotubes (TCNT) formed by bending long straight carbon nanotubes were first theoretically predicted and then experimentally observed.^{3,4} The TCNTs with all hexagonal faces usually have large strain energy and only systems with more than several thousand atoms can stably exist. However, suitably incorporating nonhexagonal defects into the hexagonal framework can release the strain energy and makes possible, though not yet experimentally proved, the existence of small stable TCNTs down to a few hundreds of atoms. It was shown that these nanotori may exhibit lower cohesive energy than spherical fullerenes^{5–8} and the effects of adding nonhexagons into hexagonal lattice on their physical properties are of great theoretical interest.^{9,10} This gives us the strong motivation to investigate the graphical problem of counting all possible isomers of small TCNTs with nonhexagonal defects.

In a report on a generalized classification scheme of high-symmetric TCNTs by Chuang et al.,¹¹ a systematic building recipe for generating graphitic toroidal structures that includes most of the previously proposed TCNT structures was proposed. The construction schemes discussed therein still have many subtleties and may be hard for one to capture due to the fact that it is difficult to manipulate the honeycomb lattice with hexagonal symmetry imposed by these graphitic related structures, as compared to the usual Euclidean rectangular coordinates system. Berger and Avron⁷ had introduced a dual space construction method for TCNTs. In their scheme, sp² carbon atoms are represented by triangular tiles, and two tiles that share a common edge are considered to have a chemical bond joining them. Particularly, they had chosen right-angled isosceles triangles to represent carbon

atoms, see Figure 1. In Figure 1a, ordinary honeycomb lattice and its dual (in dotted lines), the equilateral triangular lattice, are shown, whereas a distorted one with its dual isosceles right-angled triangular lattice are shown in (b). It is worthy to note that by making this kind of distortion on the original hexagonal lattice, the resulting tiling pattern of TCNTs in the parametric space as a whole becomes rectangular and is much easier to manipulate.

In the present report, we follow the dual space method of Berger and Avron in a more generalized way. We examine first the general construction of a D_{nh} TCNT in the dual space. Second, the chirality as commonly defined in the straight CNT is introduced. Induced chirality by twisting and shifting the original D_{nh} structure, which also leads to achiral D_{nd} TCNT, is then discussed. And finally other isomerization methods are presented and clarified within the dual space approach.

BASIC CONSTRUCTION SCHEME

As first pointed out by Tamura et al.,¹⁰ a general D_{6h} -symmetric TCNT can be constructed by gluing rectangular and isosceles trapezoidal graphene patches. Only four parametric indices are required to specify a particular D_{6h} -TCNT (Figure 2a), with one unfolded unit cell shown in Figure 2b. There are several important geometric features in this kind of TCNTs. First, the zigzag pattern always lies horizontally along the edges of the patches. Thus these TCNTs can always be decomposed into interconnected cyclic trans-polyacetylenes (PAs) of different chain lengths. We can define a latitude coordinate for each carbon atom according to which PA it belongs. Second, the length of the PA chains does not vary within the rectangular patches but increases along the radial direction in the isosceles trapezoidal patches. It is this variation that ensures the number of atoms in the inner part of the TCNT is less than the one in the outer part.

The TCNTs generated by the classification scheme developed by Berger and Avron basically share the same features. But instead of using the real space approach, they had started with a rather complicated construction method, which operates in the dual space of hexagonal honeycomb

* To whom correspondence should be addressed. E-mail: byjin@ntu.edu.tw.

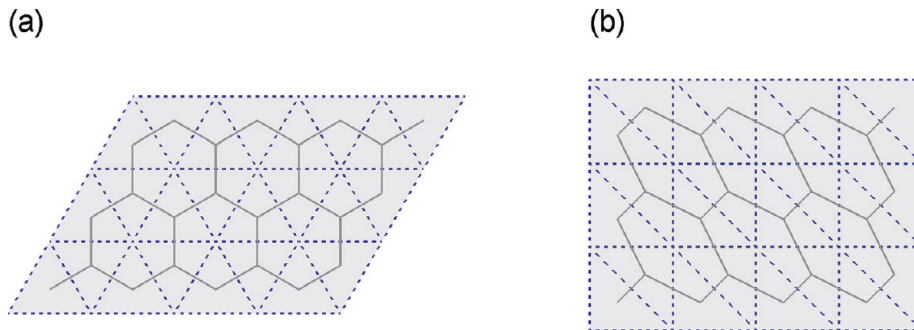


Figure 1. (a) Ordinary honeycomb lattice and its dual (dotted). (b) A distorted honeycomb with isosceles right-angled triangular tiling as its dual.

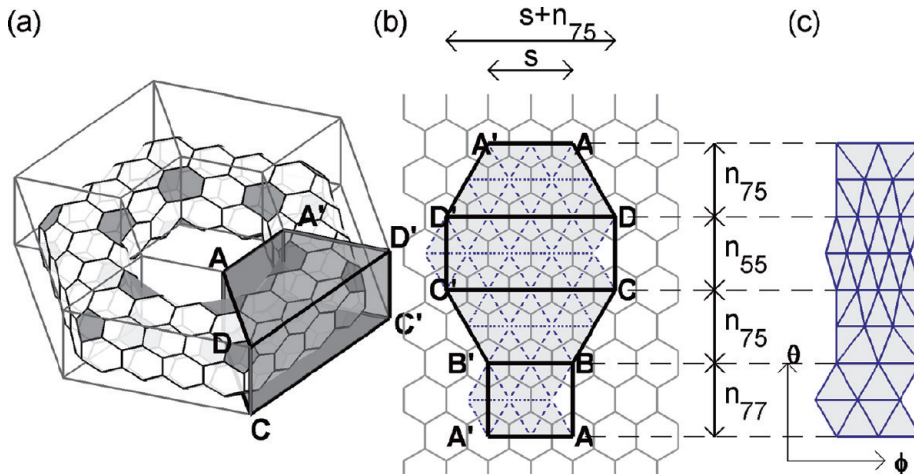


Figure 2. D_{6h} TCNT with indices $(n_{75}, n_{77}, n_{55}, s) = (2, 1, 1, 2)$. (a) Skeletal frames are drawn along the edges of a hollow-prism encompassing the TCNT, where one of the rotational symmetric unit cell is shaded and marked with capital alphabets. Nonhexagons are at the vertices of the skeletal frame and are shaded. (b) The unit cell shaded in (a) is unfolded onto planar graphene sheet. The definition of the indices are shown as the lengths of the corresponding linear segments. See text for more detailed description. The dual of the underlying honeycomb lattice, the equilateral triangular lattice, is also shown in dotted lines. One is free to choose atoms at the edge to belong to any one of the two adjacent unit cells. Here we have chosen ones at the edges $A'B'$ and $C'D'$, so these two edges bisect the triangles belonging to the unit cell whereas the two at the opposite side do not. (c) The unfolded unit cell is squeezed along the ϕ direction of the parametric plane, so the trapezoidal patches are reshaped into rectangles. The rectangular patch at the outer rim, namely, rectangle $CDD'C'$, is uniformly squeezed and remains rectangular. The tiling has constant width throughout all possible values of parameter θ .

lattice, namely the triangular lattice. In the dual space, trivalent carbon atoms are represented by triangles, and two triangles that share an edge and two vertices are identified as two bonded carbon atoms. In this scheme, isosceles right-angled triangles of different sizes are tiled onto a rectangular planar area corresponding to the (θ, ϕ) parametric plane for the toroidal surface according to certain prescribed rules. One can then dualize the resulting triangulated torus to generate the corresponding TCNT. It should be noted that this method has the advantage of bypassing the complex arithmetic it takes to specify all (hundreds to thousands or more) atoms on a 3-D object, in this case the torus. And all we need to do is merely assembling triangles of specific sizes and orientations on the parametric plane to get a unique TCNT.

However, the TCNTs classified under their rules belong to a restrictive subgroup of a wider TCNT family. In the previous paper, we have developed a generalized real-space scheme on the classification of TCNT;¹¹ in this paper, we shall demonstrate that the dual space technique can also be applied to these TCNTs, with certain modifications. In Figure 2b, we show the real and dual space representations of an unfolded unit cell for the polygonal D_{6h} TCNT in Figure 2a. In Figure 2c, the triangles representing the trivalent carbon atoms are distorted and squeezed along the ϕ

direction, following Berger and Avron's notation, so that the width of the whole triangular tiling remains the same for different latitude coordinates. Note that the two rectangular patches, besides a uniform stretching, retain their shapes while the two isosceles trapezoids are reshaped into rectangular ones. Here let us recapitulate the definitions of the parametric indices:^{10,11} n_{75} the number of strips contained in one distorted trapezoid, n_{77} half the number of strips between heptagons, n_{55} half the number of strips between pentagons, and s the number of vertical strips between heptagons. With these four parameters specified, we have constructed the dual space representation of a basic unit cell of D_{nh} -symmetric TCNT in the (θ, ϕ) plane. Repeat the basic unit cell n times, one get the whole D_{nh} -symmetric TCNT with Cartesian coordinates of the triangulated torus are given by the following:

$$\begin{aligned} x &= (R_1 - R_2 \cos \theta) \cos \phi \\ y &= (R_1 - R_2 \cos \theta) \sin \phi \\ z &= R_2 \sin \theta \end{aligned} \quad (1)$$

where R_1 and R_2 are the two radii of the torus. Position with $\theta = 0$ corresponds to the inner-rim equator, while that with $\theta = \pi$ is the outer-rim equator. The carbon atoms are located

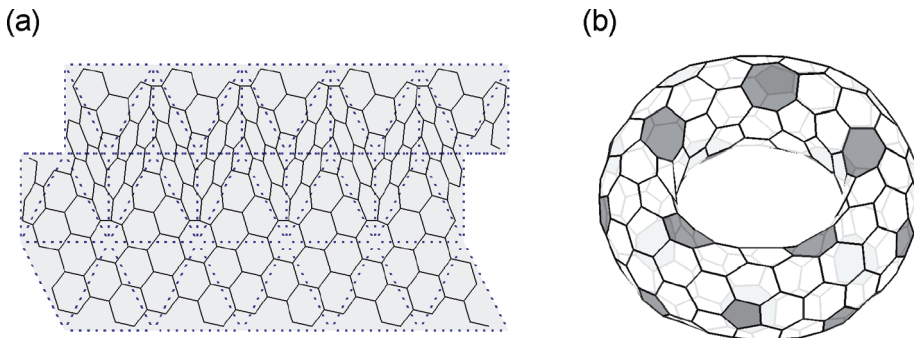


Figure 3. Goldberg inclusion. (a) The Goldberg included D_{5d} TCNT C_{40} with indices $(n_{75}, n_{77}, n_{55}, s) = (1, 0.5, 0, 1)$ by chiral vector $(2, 1)$ on the parametric plane. Triangular tiles with dotted edges are the original dual of the C_{40} , where each one of them is included with triangular graphene of chiral vector $(2, 1)$, drawn in thin black lines. Since there are seven atoms in every triangle, the resulting included TCNT is a C_{280} . (b) Optimized geometry of C_{280} .

at the centroid of each triangle, which can be obtained simply by averaging the coordinates of the three vertices of each triangle. It will become clear later that this indirect approach through the dual space representation is very useful in the classification of TCNTs.

Chirality: Goldberg Inclusion. On the basis of the ordinary polygonal D_{nh} TCNTs as given in the previous section, one can introduce the chirality, defined as in the usual convention of straight carbon nanotube,¹² to form chiral D_n TCNTs. This can be done by changing the direction of the base vector with respect to the unit vectors of honeycomb lattice, and the indices describing the TCNTs are counted as how many chiral irreducible patches it contains.¹¹ Here we present an alternative point of view from the dual space. Since each carbon atom is represented by a triangle in the dual space, we can paste a symmetric piece of triangular graphene onto each triangle to get a larger transformed TCNT as shown in Figure 3. This method was first proposed by Goldberg^{13–15} when studying a family of I_h -symmetric polyhedra, realized in physical world as fullerenes, and was applied to TCNTs by Berger and Avron and termed as the Goldberg inclusion. Note that though the physical distance between two nonhexagons are changed, their relative positions remain the same, which means the overall shape and geometric features are unchanged after Goldberg inclusions.

It can be easily shown that the number of atoms a TCNT contains is N_{tri} times larger than its parent TCNT after the Goldberg inclusion of graphitic triangles with the chiral vector (n_1, n_2) , where $N_{\text{tri}} = n_1^2 + n_2^2 + n_1 n_2$, since each atom is replaced by N_{tri} atoms in a triangle. This implies that Goldberg inclusions are special cases of the method of base vector rotation, which can be seen by comparing the formula

$$\begin{aligned} N &= n_{\text{rot}}[2N_{\text{rec}}(n_{77}s + n_{55}(n_{75} + s)) + \\ &\quad 2N_{\text{tri}}(2n_{75}s + n_{75}^2)] \\ N_{\text{rec}} &= \frac{2(n_1^2 + n_2^2 + n_1 n_2)}{\gcd(2n_1 + n_2, 2n_2 + n_1)} \\ N_{\text{tri}} &= n_1^2 + n_2^2 + n_1 n_2 \end{aligned} \quad (2)$$

where N is the total number of atoms in a rotational unit cell, N_{rec} is the number of atoms in an irreducible rectangular patch, and N_{tri} is the number of atoms in an irreducible triangular patch (for detailed description readers are referred to our previous report).¹¹ For the ordinary polygonal TCNT

defined in the very beginning, we have $(n_1, n_2) = (1, 0)$, $N_{\text{rec}} = 2$, and $N_{\text{tri}} = 1$, so it is obvious that Goldberg inclusions are the special cases of $\gcd(2n_1 + n_2, 2n_2 + n_1) = 1$. In the case when $\gcd(2n_1 + n_2, 2n_2 + n_1) = k > 1$, parameters (n_{77}, n_{55}) are scaled to k times of their original values. Here, in Figure 3b, we show the smallest chiral TCNT that can be derived from the parent D_{5d} TCNT C_{40} with indices $(1, 0.5, 0, 1)$ by the Goldberg inclusion of chiral vector $(2, 1)$.

Inner- and Outer-Rim Rotation. There is a particular variation of the ordinary polygonal D_{nh} TCNT, first described by Itoh and Ihara⁶ and was pointed out by Chuang et al.¹¹ as a rotation of the inner (outer)-rim with respect to the outer (inner)-rim of a parent TCNT. The rotation actually does not “rotate” carbon atoms but changes the way that a TCNT is cut-and-folded from the planar graphene, in the view of the real space approach utilized in our previous report. Here we shall give a different aspect of this rotation within the dual space construction scheme.

The outer part of a D_{nh} TCNT unit cell is shown on the LHS of Figure 4a, which is basically a rectangular patch of hexagons with four pentagons located at its four corners. Whereas the outer part of the corresponding TCNT unit cell after an outer-rim rotation is shown on the RHS of Figure 4a. One can see that the pentagons are switched from the corners to the middle of the rectangle. Upon closer inspection, the original arrays of regular triangles are replaced by an inhomogeneous triangular tiling, which is more densely packed along its centerline. Curiously, this inhomogeneous patch is exactly the same with the squeezed trapezoids $ADD'A'$ and $BCC'B'$ shown in Figure 2, with a different orientation. Since this operation is independent from atoms at the inner part of the torus, TCNTs with its outer-rim rotated would have pentagons and heptagons arranged in staggered conformation. An example of this kind of TCNTs is shown in Figure 5b, derived from the parent molecule shown in Figure 5a. It is worth mentioning that the original parent TCNT has zigzag patterns along its horizontal direction throughout the whole toroidal surface. However, after the outer-rim transformation is performed, the resulting TCNT has the armchair pattern in the outer part and the inner part remains unchanged.

Similarly, the rim rotation performed on the inner side of a torus leads to the switching of heptagons’s positions. This is schematically illustrated in Figure 4b, and the TCNT shown in Figure 5c is given as an example. Contrary to the outer-rim rotated version, the zigzag and armchair patterns

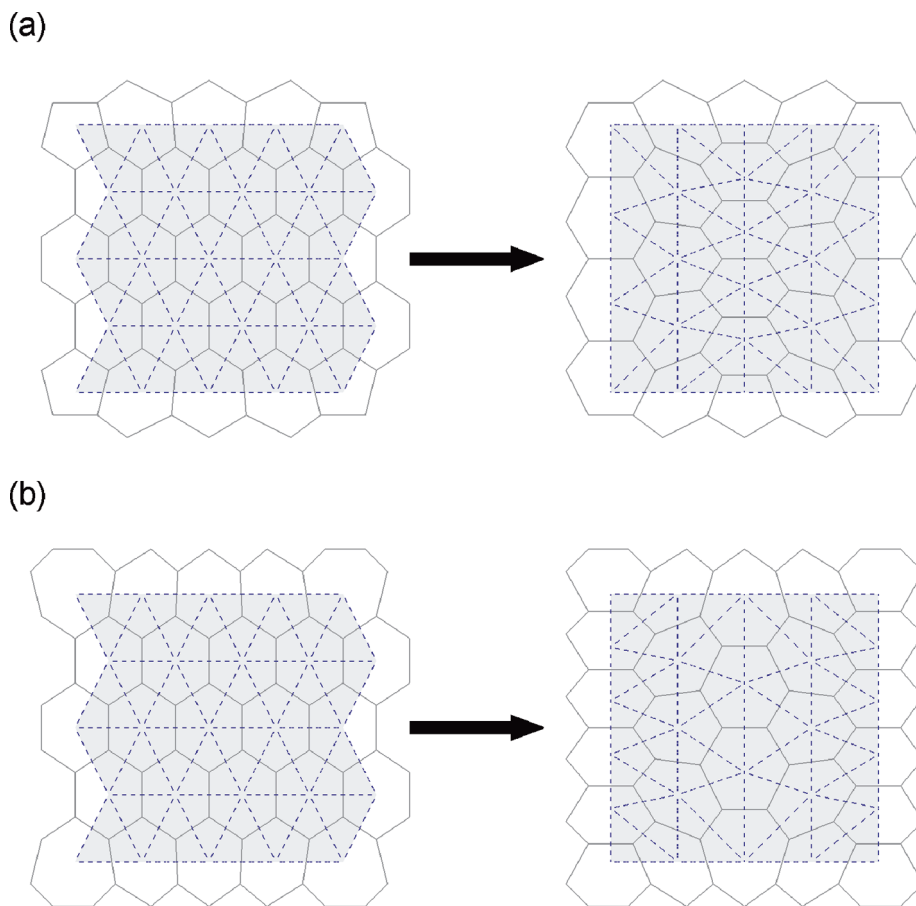


Figure 4. Illustration of rim rotation. The duals of the altered carbon atoms are drawn in dotted lines. (a) Outer-rim rotation switches the locations of pentagons from the corners to the centerline, retaining the mirror symmetries. (b) Inner-rim rotations switch the locations of heptagons in a similar fashion.

can be seen at the outer and the inner parts, respectively. Here, we would like to emphasize that in the above two cases with only inner- or outer-rim rotated, it is not possible to divide these TCNTs into interconnecting PA chains. We proceed to show one example with both of its rims rotated in Figure 5d. The molecule as a whole possesses armchair pattern, and the pentagons and heptagons therein are of eclipsed conformation similar to the original parent molecule (Figure 5a). Interestingly, the cyclic PA division of this TCNT again becomes available. But unlike the *trans*-PAs in the original parent molecule, here they are composed of interconnected *cis*-PAs.

We note that if both n_{75} and s are even numbers and both n_{77} and n_{55} are multiples of three divided by two, TCNTs with both rims rotated can be viewed as the Goldberg inclusion of a smaller parent TCNT by chiral vector (1,1), which is sometimes called a *leapfrog* transformation. In Figure 6a, the dual of a TCNT of this kind is drawn in solid (blue) lines whereas the corresponding smaller TCNT before leapfrog is drawn in dotted lines with circles on the vertices. Notice that each of the dotted triangles contains a vertex shared by six solid triangles. And this is the dual space representation of leapfrog transformation. The resulting molecules before and after the leapfrog transformation of this particular example are shown in Figure 6b and c. These two D_{5h} TCNTs have 90 and 270 carbon atoms, respectively. Though the number of atoms is augmented by three times, the relative positions of nonhexagons

remain unchanged, since the leapfrog transformation is a special case of Goldberg inclusion.

ISOMERIZATIONS

The dual space method is particularly useful when considering various isomerization processes described in the literature.^{6,7,11,16} We proceed to show how the numerous geometric variation schemes proposed earlier can be easily understood and visualized in the dual space. Hereafter we follow the notation convention used in our previous report.¹¹

Horizontal Shifting: D_{nd} Isomers. A D_{nd} -symmetric TCNT can be derived from a parent D_{nh} TCNT by suitably shifting the relative positions of the nonhexagons, while all the atoms retain their latitudes (θ), i.e. the shifting changes the connectivities between the PA chains but not themselves. In the dual space, we start with a stepwise routine construction of a D_{nd} TCNT from its D_{nh} parent molecule as shown in Figure 5a. In Figure 5a, the five upper pentagons pair up with the five lower ones (the eclipsed conformation), and so are the heptagons. Note particularly that triangles are not distorted to match the toroidal boundary conditions, as compared to the inner-shifted case of Figure 7a, where the heptagons are shifted to possess staggered conformation and the pentagons remain eclipsed. This is called an *inner-shift*. Next, consecutive, oppositely directed *outer-shift* were done in Figure 7b and c, and the pentagons are now in staggered positions and results in a D_{5d} -symmetric TCNT. It appears that Berger and Avron⁷ were the first to describe such shifting

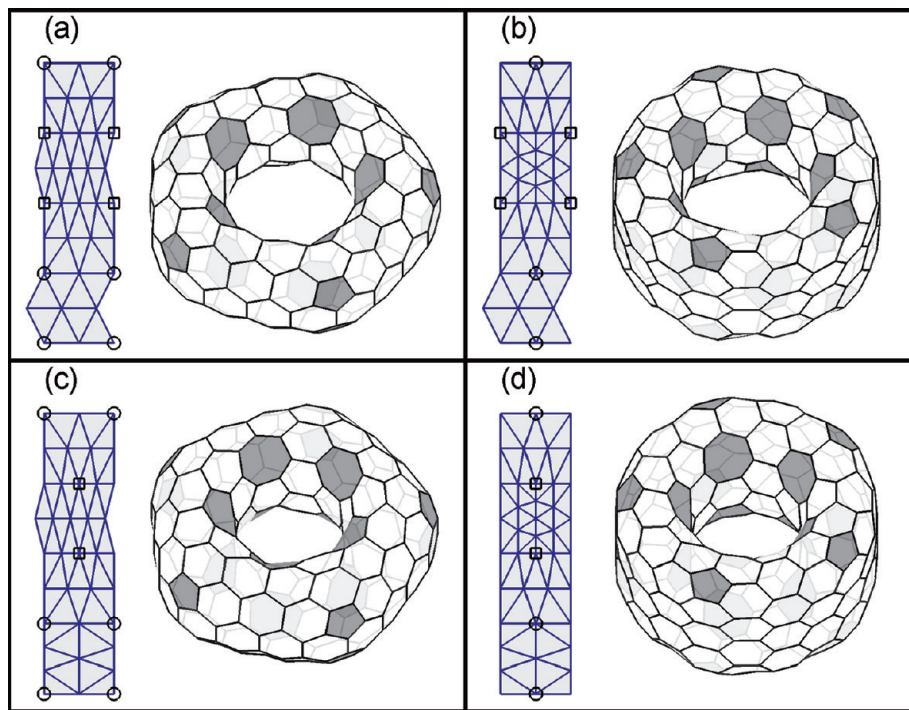


Figure 5. Rim rotation. (a) The original D_{5h} -symmetric TCNT C_{240} with indices $(2,1,1,2)$. One of the dual of its unit cells is drawn on the left and the optimized structure on the right. The locations of the pentagons are marked with squares and the heptagons with circles. (b) Outer-rim rotated version of the one shown in (a) C_{280} . The outer-rim has armchair pattern while the inner-rim remains the zigzag pattern. The rectangular patch at the outer-rim is replaced by two trapezoidal patches. (c) Inner-rim rotated version of the one shown in (a) C_{250} . The heptagons are in staggered conformation with respect to the pentagons, and the inner-rim has armchair pattern. The lower part of the unit cell on the left is replaced by two trapezoidal patches with opposite orientation. (d) TCNT with both rims rotated, C_{290} . These two transformations are independent. The TCNT as a whole has armchair pattern along its latitudes.

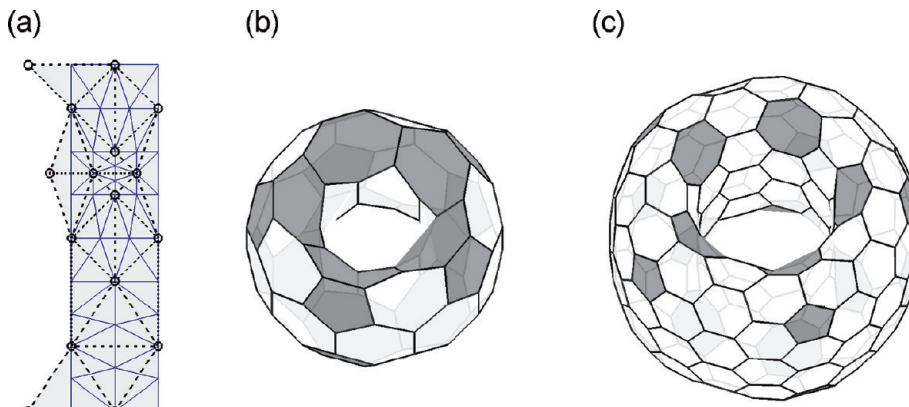


Figure 6. Equivalence of rotations of both rims and leapfrog. When n_{75} and s are even numbers and n_{77} and n_{55} are multiples of three divided by two, rotations of both rims are equivalent to leapfrog transformation. (a) The smallest nontrivial example of the equivalence. Solid (blue) triangular tiling is the dual of TCNT with $(n_{75}, n_{77}, n_{55}, s) = (2, 1.5, 1.5, 2)$ and both rims rotated. Dotted triangles are the dual of the TCNT before the leapfrog takes place, with circles marked on their vertices. (b) D_{5h} TCNT C_{90} before the leapfrog. (c) D_{5h} TCNT C_{270} after the leapfrog.

transformation, but they did not proceed to show how the shifts result in isomerization between D_{nh} and D_{nd} TCNTs. We emphasize here that for the high-symmetric D_{nd} isomer to exist, there are two restrictions on the parities of the four parametric indices. First, s and $2n_{77}$ must have the same parity, so that we can always arrange the heptagons in staggered positions. And second, $s + n_{75}$ and n_{55} must also have the same parity, so that pentagons can find their positions staggered. These have left us with only four combinations of the index parities, namely $(n_{75}, 2n_{77}, 2n_{55}, s) = (e, e, e, e), (o, o, e, o), (o, e, o, e)$, and (e, o, o, o) , where e and o stand for even and odd.

Generalized Stone–Wales Transformation. Stone and Wales¹⁶ proposed an isomerization scheme that switches the locations of two pairs of pentagons and hexagons in spherical fullerenes, which is commonly called the Stone–Wales transformation (SWT) as shown in Figure 8a. In the standard SWT, the orientation of two carbon atoms are switched, resulting in the switching of two pairs of pentagons and hexagons with the remaining molecular graph unchanged. Following Berger and Avron,⁷ here we deliberately distort the honeycomb structure such that in dual space the trivalent carbon atoms are represented by right-angled isosceles triangles (dotted blue). Thus the SWT can be seen as

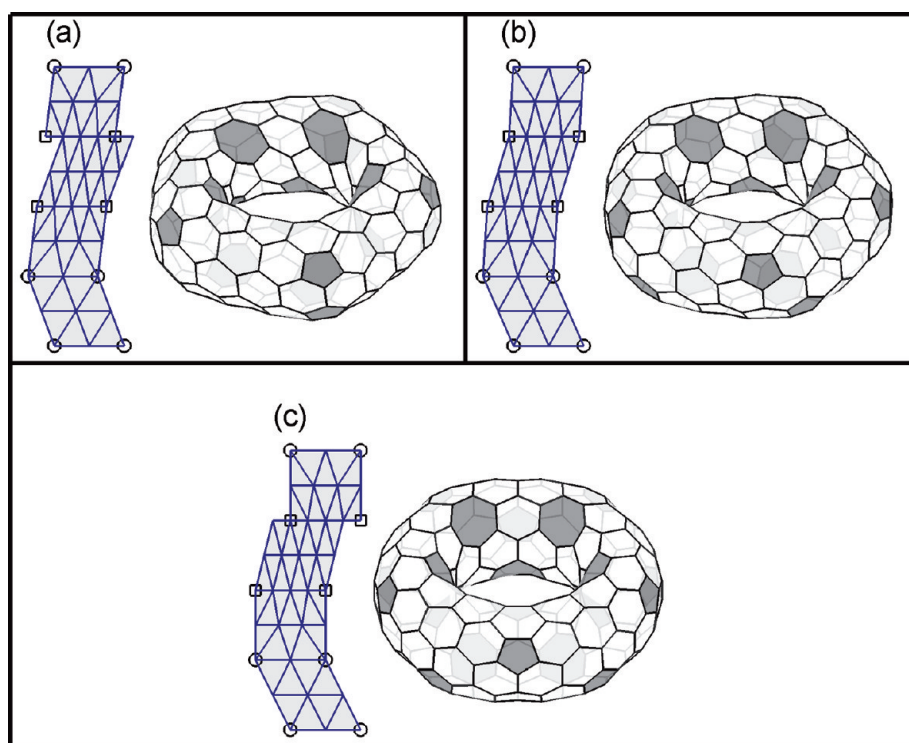


Figure 7. Horizontal shifting. The shifting transformation is applied to the TCNT C_{240} shown in Figure 5a. This transformation changes the relative latitudinal coordinates of different strips of PAs, but it does not change the number of atoms. (a) TCNT with inner-rim shifted, with its inner-shift parameter $is = 1$. The heptagons are themselves in staggered conformation while the pentagons remain eclipsed so the whole molecule suffers great torsional strain. The corresponding dual graph is distorted to match the toroidal boundary condition, as shown on the left, with pentagons marked with squares and heptagons with circles. (b) TCNT in (a) with a further outer-shift (os) on the opposite direction. This conformation is denoted as $(is, os) = (1, -1)$. The pentagons deviate from the eclipsed conformation, but they are not staggered either. (c) One more outer-shift makes the pentagons in staggered conformation. This molecule possesses D_{5d} symmetry and is denoted as $(is, os) = (1, -2)$.

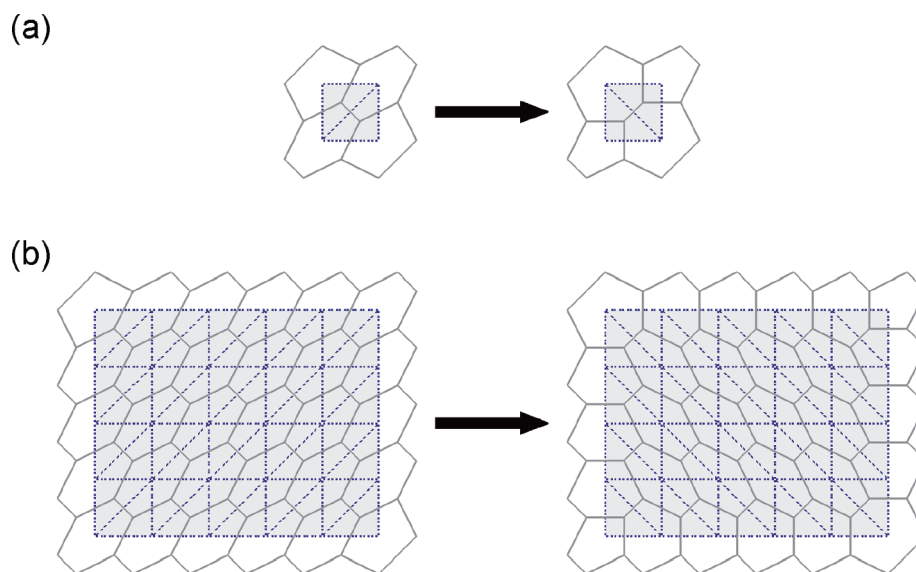


Figure 8. Stone–Wales transformation and its generalized form. The duals of the altered atoms are drawn in dotted lines. (a) The original definition of the SWT. The relative positions of a pentagon pair and a hexagon pair are switched. This corresponds in dual space as the change of orientation of a pair of triangles. (b) In gSWT, the orientations of m -by- n pairs of triangles are changed, resulting in the change of valencies of relatively distant pairs of pentagons and hexagons. In this particular case the pentagons at the upper left and lower right corners on the LHS are switched to the upper right and lower left corners on the RHS.

reflecting a pair of triangles in the dual space. In Figure 8b, we generalize this transformation, denoted as gSWT,¹¹ such that the orientations of all m -by- n pairs of triangles are switched simultaneously, in contrary to the standard SWT which changes only one pair. Similar to the effect of the standard SWT, the two pentagons located at the upper left

and lower right corners on the LHS of rectangle in Figure 8b are switched to the upper right and lower left corners. In the language of graph theory, the gSWT simultaneously reduces the valencies of two nodes by unity and increases the valencies of other two by unity, leaving the rest of the nodes in the graph with unchanged valencies.

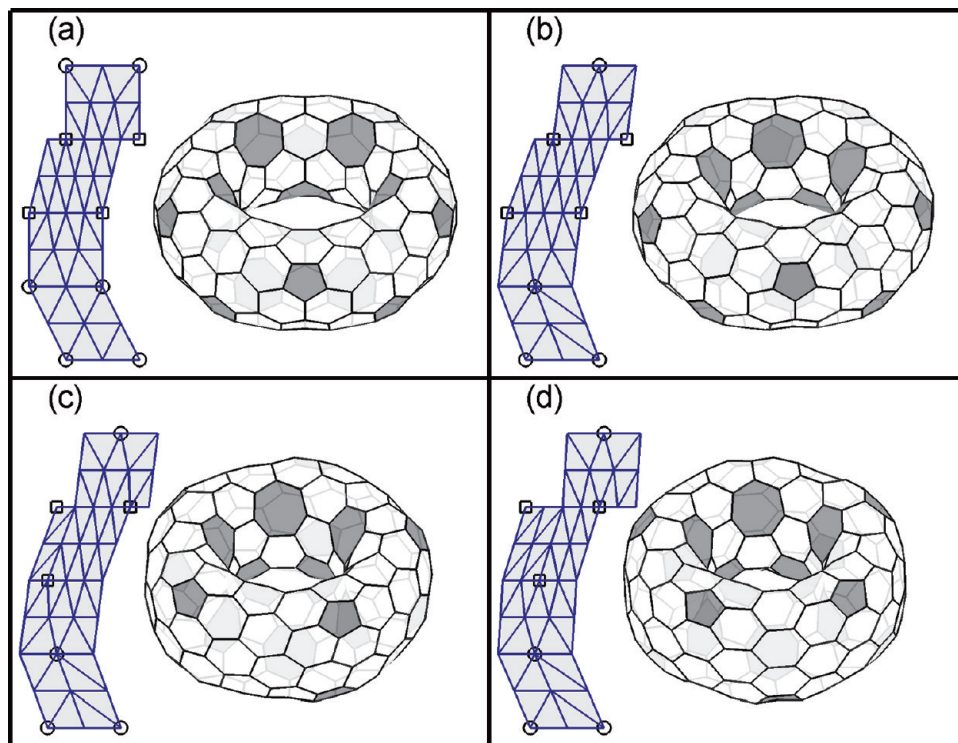


Figure 9. Effect of generalized Stone–Wales transformation on C_{240} . This isomerization changes the relative longitudinal coordinates (ϕ) of pairs of nonhexagons. The D_{5d} TCNT shown in (a) is replicated from the one shown in Figure 7c. (b) With respect to the dual shown in (a) the two pairs of triangles at the bottom right have their orientations switched. This makes the heptagons shift to the middle of their neighboring pentagons, that is, the heptagons and the pentagons are in staggered conformation. This molecule is denoted as $i\text{SWT} = 1$. (c) Continuing from (b) the two pairs of triangles at the upper left switch their directions. The pentagons deviate from the high symmetric points resulting in a chiral molecule. This molecule is denoted as $(i\text{SWT}, o\text{SWT}) = (1,1)$. (d) Continuing from (c) another two pairs of triangles switch their directions. The pentagons are again located at high symmetric points, and the nonhexagons are in eclipsed conformation. The whole molecule as a whole possesses armchair pattern similar to the case shown in Figure 5d. This molecule is denoted as $(i\text{SWT}, o\text{SWT}) = (1,2)$.

To see the actual effect that the gSWT can produce on a TCNT in the dual space, here we give a detailed examination of the gSWT on the D_{5h} -TCNT as shown in Figure 9a (replicated from Figure 7c for convenience). In Figure 9b the two pairs of triangles at the lower right have their orientations switched with respect to the parent TCNT in Figure 9a. The positions of the heptagons are switched to the positions of their hexagonal neighbors. Since the heptagons remain staggered, the resulting TCNT isomer in Figure 9b also belongs to the D_{nd} point group. We denote this action as $i\text{SWT}$ for inner-rim gSWT, and in this case $i\text{SWT} = 1$ because it switches 1-by- $2n_{77}$ pairs of triangles.

We next make a further gSWT on the outer-rim, see Figure 9c, where two pairs of triangles at the upper left have switched their orientations. This transformation brings the pentagons not only close to one of the heptagons but also further apart from the other heptagon, leading to a chiral TCNT.⁹ Likewise, we denote this TCNT with $(i\text{SWT}, o\text{SWT}) = (1,1)$, where $o\text{SWT}$ stands for the outer-rim gSWT. In Figure 9d, we show the structure corresponding to a transformed isomer with $(i\text{SWT}, o\text{SWT}) = (1,2)$. Interestingly, in this isomer, the pentagons are switched to the other sets of high-symmetry lines (longitudes) of D_{nd} point group, thus this transformed TCNT become achiral again. As readers

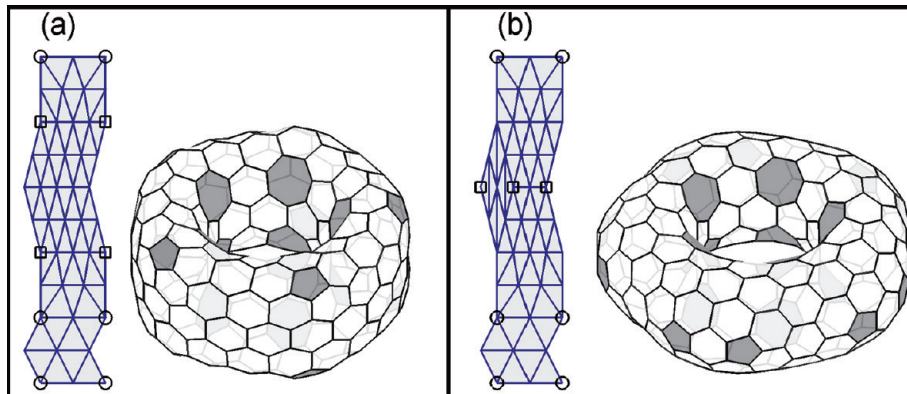


Figure 10. Generalized Stone–Wales transformation applied to D_{5h} TCNT. (a) Original D_{5h} TCNT C_{320} with indices $(n_{75}, n_{77}, n_{55}, s) = (2, 1, 2, 2)$. (b) A gSWT is applied at the outer-rim. Different from the one applied to the D_{nd} cases in Figure 8, this gSWT switches the pentagons to the outer equator. The resulting TCNT is still of D_{5h} symmetry. As can be seen from the dual graph on the left, directions of four pairs of triangles, forming a parallelogram, are switched.

might notice, similar to the D_{nh} TCNTs with both inner-rim and outer-rim rotated, this molecule can be seen as the interconnected *cis*-PA chains. We emphasize here that the gSWT is in fact equivalent to the application of rim rotation to D_{nd} cases. However, the gSWT cannot be applied to TCNTs with D_{nh} symmetry, for it produces additional nonhexagons other than the $2n$ pairs at the outset. It is only in the real space that these two cases look the same but they bear no resemblance in the view of the dual space method. If two more pairs of triangles are switched in this case, that is, $(i\text{SWT}, o\text{SWT}) = (1,3)$, the corresponding D_5 TCNT is enantiomeric to the one shown in Figure 9c. In general, (a,b) -isomer forms enantiomeric pairs with $(s-a, b)$ - or $(a, n_{75} + s - b)$ -isomer, where the latter two are diastereomers.

The gSWT isomers of a D_{nd} TCNT can be D_{nd} as well only when certain parity restrictions on the indices are held. We are not intended to give the detailed derivation of them since this is not particularly illuminating. Readers of interest are referred to the table and the Supporting Information in our previous paper¹¹ for figures of their real space geometries.

Although we have stated that the gSWT cannot be applied to D_{nh} TCNTs, this is not quite true if we apply this transformation in a different way. For instance, in Figure 10(a), a typical D_{5h} TCNT is drawn, and in (b), four pairs of triangles at the upper-left forming a parallelogram are transformed by the gSWT. The resulting TCNT still possesses D_{5h} symmetry but have all pentagons located at the outer equator of the torus and again the latitude coordinates are not well-defined. Since we have the symmetry of reflection through xy -plane, that is, the σ_h symmetry element, this kind of gSWT always involves the switching of n_{55}^2 pairs of triangles, which form a rhombus in a unit cell. As a result, when $n_{55} = n_{75} + s$, the kind of gSWT will merge n pairs of pentagons into n quadrilaterals at the outer equator. However, gSWT of this kind cannot be applied to the inner-rim heptagons for it creates additional nonhexagons.

Finally, we would like to stress that the inner-rim or “neck” structures are of particular importance because we can use them as the fundamental building blocks for constructing other forms of graphitic cages with different topologies, especially fullerenes with genus number greater than unity, for example, double torus, or other high-genus carbon nanostructures. Moreover, the isomerization methods we have described above change only the relative arrangement of carbon atoms in a “neck” structure locally. This means that the classification scheme we introduced in this and previous papers can in principle be extended to other complicated graphitic structures.¹¹

CONCLUSION

In this paper, we apply the dual space technique to a wide family of TCNT structures described in the literature. We

show that this method is particularly useful in discussing numerous complicated problems of geometrical and graphical variation of honeycomb lattice. Many of the previously proposed geometric variation methods of TCNTs, including Goldberg inclusions, rim rotation, horizontal shifting and generalized Stone-Wales transformation, are clarified and rationalized in the view of dual space on the (θ, ϕ) parametric plane. Manifested chirality induced by these transformations and the criteria of existence for highly symmetric D_{nd} isomers are also discussed. The full power of the dual space representation will become transparent when one considers more complicated 3D structures such as high-genus fullerenes and periodic Schwarzites.

ACKNOWLEDGMENT

We wish to acknowledge the financial support of NSC, Taiwan, ROC.

REFERENCES AND NOTES

- Kroto, W.; Heath, J.; O'Brien, S.; Curl, R.; Smalley, R. C₆₀ Buckminsterfullerene. *Nature* **1985**, *318*, 162–163.
- Iijima, S. Helical microtubules of graphitic carbon. *Nature* **1991**, *354*, 56–58.
- Liu, J.; Dai, H.; Hafner, J. H.; Colbert, D. T.; Smalley, R. E.; Tans, S. J.; Dekker, C. Fullerene “crop circles”. *Nature* **1997**, *385*, 780–781.
- Ahlskog, M.; Seynaeve, E.; Vullers, R. J. M.; Van Haesendonck, C.; Fonseca, A.; Hernadi, K.; Nagy, J. B. Ring formation from catalytically synthesized carbon nanotubes. *Chem. Phys. Lett.* **1999**, *300*, 202–206.
- Itoh, S.; Ihara, S.; Kitakami, J. Toroidal form of carbon C₃₆₀. *Phys. Rev. B* **1993**, *47*, 1703–1704.
- Itoh, S.; Ihara, S. Isomers of the toroidal forms of graphitic carbon. *Phys. Rev. B* **1994**, *49*, 13970–13974.
- Berger, J.; Avron, J. E. Classification scheme for toroidal molecules. *J. Chem. Soc., Faraday Trans.* **1995**, *91*, 4037–4045.
- Oh, D.; Park, J. M.; Kim, K. S. Structures and electronic properties of small carbon nanotube tori. *Phys. Rev. B* **2000**, *62*, 1600–1603.
- Ceulemans, A.; Chibotaru, L. F.; Fowler, P. W. Molecular anapole moments. *Phys. Rev. Lett.* **1998**, *80*, 1861–1864.
- Tamura, R.; Ikuta, M.; Hirahara, T.; Tsukada, M. Positive magnetic susceptibility in polygonal nanotube tori. *Phys. Rev. B* **2005**, *71*, 045418.
- Chuang, C.; Fan, Y. C.; Jin, B. Y. Generalized classification scheme of toroidal and helical carbon nanotubes. *J. Chem. Inf. Model.* **2009**, *49*, 361–368.
- Saito, R.; Dresselhaus, G.; Dresselhaus, M. In *Physical Properties of Carbon Nanotubes*, 1st ed.; World Scientific Publishing Company: Singapore, 1998; pp 35–58.
- Goldberg, M. A class of multi-symmetric polyhedra. *Tohoku Math. J.* **1937**, *43*, 104–108.
- Coxeter, H. S. M. In *A Spectrum of Mathematics*, 1st ed.; Butcher, J. C., Eds.; Oxford University Press: Oxford, U.K., 1971.
- Fowler, P. W. How unusual is C₆₀? Magic numbers for carbon clusters. *Chem. Phys. Lett.* **1986**, *131*, 444–450.
- Stone, A.; Wales, D. Theoretical studies of icosahedral C₆₀ and some related species. *Chem. Phys. Lett.* **1986**, *128*, 501–503.